

A fast and accurate analysis of the interacting cracks in linear elastic solids

Dong-Feng Li · Chen-Feng Li · Si-Qi Shu ·
Zhao-Xi Wang · Jian Lu

Received: 15 July 2008 / Accepted: 17 July 2008 / Published online: 6 August 2008
© Springer Science+Business Media B.V. 2008

Abstract This paper presents a fast and accurate solution for crack interaction problems in infinite- and half- plane solids. The new solution is based on the method of complex potentials developed by Muskhelishvili for the analysis of plane linear elasticity, and it is formulated through three steps. First, the problem is decomposed into a set of basic problems, and for each sub-problem, there is only one crack in the solid. Next, after a crack-dependent conformal mapping, the modified complex potentials associated with the sub-problems are expanded into Laurent's series with unknown coefficients, which in turn provides a mechanism to exactly implement in the form of Fourier series the boundary condition in each sub-problem. Finally, taking into account the crack interaction via a perturbation approach, an iterative algorithm based on fast Fourier transforms (FFT) is developed to solve the unknown Fourier coefficients, and the solution of the whole problem is readily obtained with the superposition of the complex potentials in each sub-problem. The performance of the proposed method is fully investigated by comparing with benchmark results in the literatures, and superb accuracy and efficiency is observed in all situations including patterns where cracks are closely spaced. Also, the new method is able to cope with interactions among a large number of cracks, and this capability is demonstrated by a calculation of effective moduli of an elastic solid with thousands of randomly-spaced cracks.

Keywords Crack interaction · Complex potential · Conformal mapping · Stress intensity factor · Crack opening displacement · Effective moduli

D.-F. Li · S.-Q. Shu · Z.-X. Wang · J. Lu (✉)
Department of Mechanical Engineering, The Hong Kong Polytechnic University,
Hung Hom, Kowloon, Hong Kong
e-mail: mmmelu@inet.polyu.edu.hk

C.-F. Li
Civil and Computational Engineering Centre, School of Engineering, University of Wales Swansea,
Singleton Park, Swansea SA2 8PP, UK

1 Introduction

The knowledge about crack interactions in solid materials is of fundamental importance in understanding the toughening mechanism of crack shielding and predicting the effective moduli of cracked solids. It plays a key role in many engineering applications, for instance, design and manufacturing functional gradient materials such as TBC (Thermal Barrier Coating), and controlling the surface crack network generated in nuclear plant structures. The research of crack interactions has been in progress for several decades, and a variety of methods have been developed to tackle the problem from different viewpoints and with different emphases. As a powerful analysis tool for linear elasticity plane problems, the complex potential representation developed by [Muskhelishvili \(1953a\)](#) has been widely employed in the study of crack interactions.

The analytical solutions (e.g. [Muskhelishvili 1953a](#); [Westergaard 1939](#); [Willmore 1949](#); [Koiter 1959](#); [Erdogan 1962](#); [Sih 1964](#)) for some simple arrays of cracks in 2D planes have been obtained for a long time. However, it is difficult to analytically solve the problem for the arbitrary array of cracks, and hence different numerical approaches have been developed. Among these numerical methods, the singular integral equation (SIE) method (e.g. [Muskhelishvili 1953b](#); [Erdogan 1969](#); [Erdogan and Gupta 1972](#)) and the boundary integral equation (BIE) method (e.g. [Chen and Chen 1995](#); [Pan 1997](#); [Denda and Dong 1997](#)) are outstanding and have demonstrated their flexibility and versatility in many crack-related problems. There are a large number of literatures related to the development and application of the SIE and BIE methods. Specially, for the SIE method, [Muskhelishvili \(1953b\)](#) first proposed the general theory, and based on Chebyshev's polynomial expansions, [Erdogan et al. \(Erdogan \(1969\), Erdogan and Gupta \(1972\)\)](#) further developed the SIE approximate solutions for a variety of crack-related problems. For the BIE method, which is based on Green's functions, its numerical solutions were developed using the boundary element method (BEM) (e.g. [Chen and Chen 1995](#); [Pan 1997](#); [Denda and Dong 1997](#)). Moreover, by decomposing the problem into several sub-problems and treating the traction on the surface of crack in each sub-problem as an unknown function, [Kachanov \(1987\)](#) presented a simple method to calculate the Stress Intensity Factors (SIFs) for problems containing irregularly distributed cracks. Later, [Benveniste et al. \(1989\)](#) generalized Kachanov's method in 2D cases by approximating of the real traction on a given crack with some artificial stresses generated by other cracks which are constructed from some lower-order Legendre polynomials. [Li et al. \(2003\)](#) decomposed the crack traction into a linear term and a non-linear component, in which only the interaction of the linear term is considered; however, the linear term in Li's method is in equilibrium with the Kachanov traction but not the real crack traction on the crack surface. By combining the Kachanov's method with the effective stress field methods, [Feng et al. \(2003\)](#) and [Ma et al. \(2004\)](#) proposed a simple method to analysis the interaction of a large number of cracks.

For the polynomial approximation techniques, [Kachanov \(2003\)](#) gives a review, in which it is pointed that formidable computational difficulties are encountered when considering closely-spaced cracks. Another computational difficulty in the above numerical methods is in coping with a large number of interacting cracks. In these methods, the computational cost is mainly spent on calculating the numerical integrations on the crack segments and on solving the induced linear algebraic systems. Hence, in a problem with a large number of cracks, (a) the non-sparse matrix of the system of linear algebraic equations for the problem will cause trouble in data storage; (b) the number of computational operations increases significantly since it is generally proportional to the square of the number of cracks.

In order to overcome the above computational difficulties encountered in the analysis of crack interactions, a new method is developed in this paper. First, following Muskhelishvili’s approach, two complex potentials are defined for the multiple-crack interaction problem to describe the displacement field, stress field and corresponding stress boundary conditions. Then, these two complex potentials are decomposed into the sum of a sequence of complex functions. This is equivalent to treat the multiple-crack interaction problem as a superposition of a set of simpler problems, and for each sub-problem, there is only one crack in the solid. After a conformal mapping, the complex functions in each sub-problem are expressed in the form of Laurent’s series expansions, which in turn provides a natural way for each sub-problem to represent with Fourier series the boundary condition on the surface of the crack. Thus, the problem of multiple-crack interaction is reduced to determining the unknown Fourier coefficients. Finally, an accelerated iterative algorithm is developed with assistance of FFT to solve the unknown constants, and the mutual influences among cracks are taken into account. The proposed method can be extended with minor modifications to solve the problem of half-plane containing internal cracks, since the conformal mappings of half-plane and the conformal mapping of crack induce formally-similar boundary conditions.

2 Statement of problem

As shown in Fig. 1, many crack-interaction problems encountered in engineering practice can be modeled as an infinite isotropic elastic plate containing multiple straight cracks and bearing stresses at infinity. In practical problems, due to thermal loads and residual stresses etc. in the solid, there may be induced external loads on the crack surfaces as well.

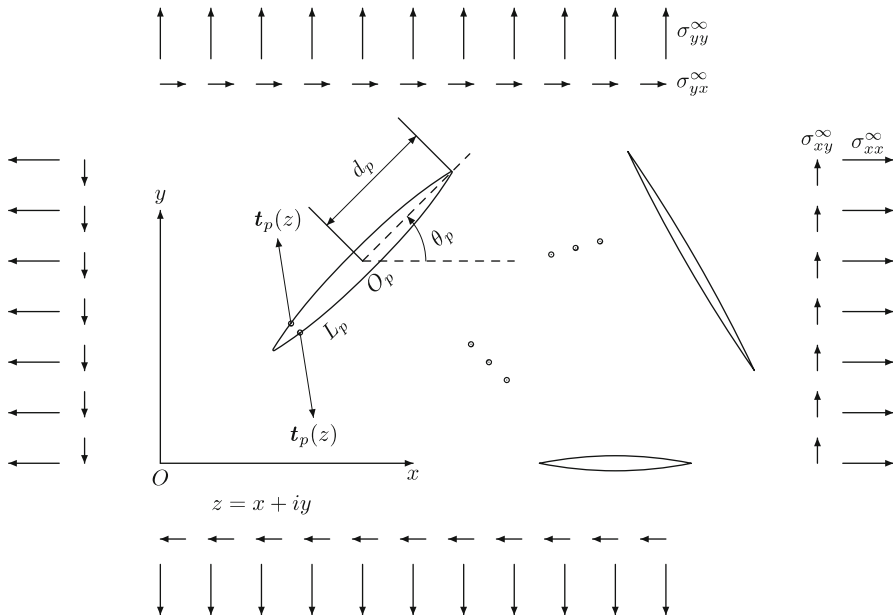


Fig. 1 An infinite plate containing multiple cracks

In the complex analysis theory of plane elasticity, [Muskhelishvili \(1953a\)](#) shows that the problem can always be solved by seeking two complex functions $\varphi(z)$ and $\psi(z)$ in the region occupied by the isotropic elastic solid to satisfy the specified boundary conditions. Specifically, let E , μ , G denote the Young's modulus, Poisson's ratio and shear modulus respectively, the displacement field $\mathbf{u}(z)$ and the stress field $\boldsymbol{\sigma}(z)$ can be expressed as

$$2G(u_x + iu_y) = \kappa\varphi(z) - z\overline{\varphi'(z)} - \overline{\psi(z)}, \quad (1a)$$

$$\sigma_{xx} + \sigma_{yy} = 2 \left[\varphi'(z) + \overline{\varphi'(z)} \right], \quad (1b)$$

$$\sigma_{yy} - \sigma_{xx} + 2i\sigma_{xy} = 2 \left[\overline{z}\varphi''(z) + \psi'(z) \right], \quad (1c)$$

where $\kappa = 3 - 4\nu$ for plane strain and $\kappa = \frac{3-\nu}{1+\nu}$ for plane stress. Moreover, for the problem shown in [Fig. 1](#), if the loads applied on each crack surface are assumed to be self-balanced, then the general solution is of the form

$$\varphi(z) = \Gamma z + \varphi_0(z), \quad (2a)$$

$$\psi(z) = \Gamma' z + \psi_0(z), \quad (2b)$$

where

$$\Gamma = \frac{\sigma_{xx}^\infty + \sigma_{yy}^\infty}{4},$$

$$\Gamma' = \frac{\sigma_{yy}^\infty - \sigma_{xx}^\infty}{2} + i\sigma_{xy}^\infty$$

are constants determined by the stress at infinity, and $\varphi_0(z)$ and $\psi_0(z)$ are holomorphic in the whole plane excluding the crack segments.

The objective of present paper is to determine the two complex potentials $\varphi_0(z)$ and $\psi_0(z)$ to solve the problem in [Fig. 1](#). For a special case where all cracks are distributed along a straight line, [Muskhelishvili \(1953a\)](#) has obtained the exact solution. However, if the cracks are irregularly distributed, it is generally difficult to solve the problem analytically and the approximate numerical approaches should be adopted instead.

3 The analytical approach

3.1 Conformal mapping and boundary conditions

In order to describe the boundary condition on the crack surface as shown in [Fig. 1](#), we introduce the following conformal mapping

$$z = \omega_p(\zeta) = \frac{d_p}{2}(\zeta + \zeta^{-1})e^{i\theta_p} + z_p^0, \quad 1 \leq p \leq N, \quad (3)$$

where d_p denotes the half length of the p -th crack, θ_p the angle between the crack and the x -axis, and z_p^0 the complex coordinate of the central point O_p of the p -th crack. For any fixed integer p , [Eq. 3](#) maps the exterior of the p -th crack in z -plane to the exterior of the unit circle in ζ -plane and the crack tips are mapped to $\zeta = \pm 1$.

In the curvilinear coordinate system induced by Eq.3 and $\zeta = \rho e^{i\vartheta}$, the stress components can be expressed as (see Muskhelishvili (1953a))

$$\sigma_{\rho\rho} + \sigma_{\vartheta\vartheta} = 2 \left[\varphi'(z) + \overline{\varphi'(z)} \right], \tag{4a}$$

$$\sigma_{\vartheta\vartheta} - \sigma_{\rho\rho} + 2i\sigma_{\rho\vartheta} = \frac{2\zeta^2 \omega_p'(\zeta)}{\rho^2 \omega_p'(\zeta)} \left[\overline{z} \varphi''(z) + \psi'(z) \right]. \tag{4b}$$

Let $\rho \rightarrow 1$, which implies $\zeta \rightarrow e^{i\vartheta}$ and $\frac{\zeta^2 \omega_p'(\zeta)}{\rho^2 \omega_p'(\zeta)} \rightarrow -e^{2i\theta_p}$, then the stress on the boundary of the p -th crack can be described as

$$\sigma_{\rho\rho} - i\sigma_{\rho\vartheta} = \overline{\varphi'(z)} + \Omega'(z; \theta_p, z_p^0, \varphi, \psi), \text{ on } |\zeta| = 1, \tag{5}$$

where

$$\Omega(z; \theta_p, z_p^0, \varphi, \psi) = e^{2i\theta_p} \psi(z) + \left(z - z_p^0 + e^{2i\theta_p} \overline{z_p^0} \right) \varphi'(z), \tag{6}$$

which is a multi-variable function depending not only on the complex variable z , but also on the complex functions $\varphi(z)$, $\psi(z)$ and two parameters θ_p, z_p^0 . It should be noted that Ω' in Eq. 5 should be understood as the full derivative of Ω with respect to the variable z .

As shown in Fig. 1, if the crack traction $t_p(z)$ is given in terms of a complex-valued function whose real part and image part are the normal and shear traction on the crack respectively, then the boundary condition on the p -th crack surface can be described as

$$\overline{\varphi'(z)} + \Omega'(z; \theta_p, z_p^0, \varphi, \psi) = t_p(z), \text{ on } |\zeta| = 1. \tag{7}$$

Substituting Eq. 2 into Eq. 7 yields

$$\overline{\varphi_0'(z)} + \Omega'(z; \theta_p, z_p^0, \varphi_0, \psi_0) = t_p(z) - (\Gamma + \overline{\Gamma}) - e^{2i\theta_p} \Gamma', \text{ on } |\zeta| = 1. \tag{8}$$

Equation 8 is the summarizing equation that defines the boundary condition on the p -th crack in terms of the unknown complex potentials $\varphi_0(z)$ and $\psi_0(z)$.

3.2 The superposition principle

Since the functions $\varphi_0(z)$ and $\psi_0(z)$ are sectionally holomorphic, they can be represented by two Cauchy type integrals on the path $\bigcup_{q=1}^N L_q$ (see Muskhelishvili (1953b)), where L_q denotes the path occupied by the q -th crack segment. Hence, after decomposing the Cauchy type integral into the sum of integrals on each individual crack path, the unknown complex potentials $\varphi_0(z), \psi_0(z)$ can be expressed as

$$\varphi_0(z) = \sum_{q=1}^N \varphi_q(z), \tag{9a}$$

$$\psi_0(z) = \sum_{q=1}^N \psi_q(z), \tag{9b}$$

where $\varphi_q(z)$ and $\psi_q(z)$ are holomorphic functions in the whole plane excluding the q -th crack segment. In addition, based on Eqs. 6 and 9, function $\Omega(z; \theta_p, z_p^0, \varphi_0, \psi_0)$ can be written as

$$\Omega(z; \theta_p, z_p^0, \varphi_0, \psi_0) = \sum_{q=1}^N \Omega(z; \theta_p, z_p^0, \varphi_q, \psi_q), \quad 1 \leq p \leq N. \tag{10}$$

The above decompositions in Eqs. 9 and 10 also hold for the derivatives of these functions.

The physical meaning of Eq. 9 is the well known superposition principle of crack interactions. That is, the problem of N -crack interactions can be regarded as a superposition of N simple sub-problems each containing a single crack subjected to unknown tractions on its boundary and zero stress at infinity (see Kachanov 1987). From this point of view, functions $\varphi_q(z)$ and $\psi_q(z)$ are the complex potentials in the sub-problem associated with the q -th crack.

3.3 Series representation of the complex functions

After applying the conformal mapping $z = \omega_q(\zeta)$, which maps the exterior of the q -th crack in z -plane to the exterior of the unit circle in ζ -plane, functions $\varphi_q(\omega_q(\zeta))$, $\psi_q(\omega_q(\zeta))$ and their derivatives are all holomorphic in the exterior of the unit circle in ζ -plane, and so are the function $\Omega(\omega_q(\zeta); \theta_q, z_q^0, \varphi_q, \psi_q)$ and its derivative. Hence functions φ_q' and Ω' can be expanded into Laurent series

$$\varphi_q'(\omega_q(\zeta)) = \frac{e^{i\theta_q}}{\zeta \omega_q'(\zeta)} \sum_{n=1}^{\infty} A_n^q \zeta^{-n}, \quad 1 \leq q \leq N, \tag{11a}$$

$$\Omega'(\omega_q(\zeta); \theta_q, z_q^0, \varphi_q, \psi_q) = \frac{e^{i\theta_q}}{\zeta \omega_q'(\zeta)} \sum_{n=1}^{\infty} B_n^q \zeta^{-n}, \quad 1 \leq q \leq N, \tag{11b}$$

where A_n^q, B_n^q are unknown complex constants.

Next, in order to represent the crack boundary condition Eq. 8 in a series form, functions $\varphi_q'(\omega_p(\zeta))$ and $\Omega'(\omega_p(\zeta); \theta_p, z_p^0, \varphi_q, \psi_q)$ are reorganized as follows

$$\varphi_q'(\omega_p(\zeta)) = \frac{e^{i\theta_p}}{\zeta \omega_p'(\zeta)} \sum_{n=1}^{\infty} A_n^q \eta_n^{qp}(\zeta), \tag{12a}$$

$$\Omega'(\omega_p(\zeta); \theta_p, z_p^0, \varphi_q, \psi_q) = \frac{e^{i\theta_p}}{\zeta \omega_p'(\zeta)} \sum_{n=1}^{\infty} [A_n^q \chi_n^{qp}(\zeta) + B_n^q \mu_n^{qp}(\zeta)], \tag{12b}$$

where the detailed expressions of the functions $\eta_n^{qp}(\zeta)$, $\chi_n^{qp}(\zeta)$ and $\mu_n^{qp}(\zeta)$ are given in the Appendix. The derivatives $\varphi_0'(\omega_p(\zeta))$ and $\Omega'(\omega_p(\zeta); \theta_p, z_p^0, \varphi_0, \psi_0)$, thus, can be expressed in a series form by substituting the Eqs. 11 and 12 into their decomposition formulae that are similar with Eqs. 9a and 10.

Finally, multiplying $\zeta \omega_p'(\zeta)$ on both sides of Eq. 8, the boundary condition on the surface of the p -th crack can be described as

$$\begin{aligned} & \sum_{n=1}^{\infty} \left(B_n^p e^{-in\vartheta} - \overline{A_n^p} e^{in\vartheta} \right) \\ & = b_p(\vartheta) - \sum_{\substack{q=1 \\ q \neq p}}^N \sum_{n=1}^{\infty} \left[A_n^q \chi_n^{qp}(e^{i\vartheta}) + B_n^q \mu_n^{qp}(e^{i\vartheta}) - \overline{A_n^q \chi_n^{qp}(e^{i\vartheta})} \right], \end{aligned} \tag{13}$$

where A_n^q and B_n^q are the unknown constants and

$$b_p(\vartheta) = e^{i(\vartheta-\theta_p)} \omega_p'(e^{i\vartheta}) [t_p(\omega_p(e^{i\vartheta})) - (\Gamma + \overline{\Gamma}) - e^{2i\theta_p} \Gamma']. \tag{14}$$

The second term in the right-hand side of Eq. 13 represents the mutual influence from the other cracks to the p -th crack. Due to the complexity of this interaction term, it is generally

difficult to exactly solve Eq. 13. Hence, an explicit iterative algorithm is proposed in the next sub-section to approximately determine the unknowns A_n^p and B_n^p .

3.4 The explicit iterative solution algorithm

If the mutual effects of cracks are ignored, the unknown constants A_n^p, B_n^p can be directly obtained via Fourier integrals

$$B_n^{p(0)} = \frac{1}{2\pi} \int_0^{2\pi} b_p(\vartheta) e^{in\vartheta} d\vartheta, A_n^{p(0)} = -\frac{1}{2\pi} \int_0^{2\pi} \overline{b_p(\vartheta)} e^{in\vartheta} d\vartheta, \tag{15}$$

where the superscripts “(0)” distinguishes the approximate solution from the exact values of the unknowns. Based on Eq. 14 and taking into account the mutual interaction among cracks, the initial approximations $B_n^{p(0)}$ and $A_n^{p(0)}$ can be continuously improved to satisfy any given accuracy requirement through the following iterative procedure.

$$B_n^{p(m+1)} = B_n^{p(0)} - \frac{1}{2\pi} \int_0^{2\pi} I_p^{(m)}(\vartheta) e^{in\vartheta} d\vartheta, \tag{16a}$$

$$A_n^{p(m+1)} = A_n^{p(0)} + \frac{1}{2\pi} \int_0^{2\pi} \overline{I_p^{(m)}(\vartheta)} e^{in\vartheta} d\vartheta, \tag{16b}$$

where

$$I_p^{(m)}(\vartheta) = \sum_{\substack{q=1 \\ q \neq p}}^N \sum_{n=1}^{\infty} \left[A_n^{q(m)} \chi_n^{qp}(e^{i\vartheta}) + B_n^{q(m)} \mu_n^{qp}(e^{i\vartheta}) - \overline{A_n^{q(m)} \eta_n^{qp}(e^{i\vartheta})} \right]. \tag{17}$$

Once the unknown constants A_n^p and B_n^p are obtained, the series solutions for functions $\varphi'_p(\omega_p(\zeta))$ and $\Omega'(\omega_p(\zeta); \theta_p, z_p^0, \varphi_p, \psi_p)$ can be readily constructed according to Eq. 11, which essentially determines the complex potentials $\varphi_0(z)$ and $\psi_0(z)$.

The computational cost of the above iterative algorithm mainly includes two parts: (a) calculating the interacting functions $\eta_n^{qp}(e^{i\vartheta}), \chi_n^{qp}(e^{i\vartheta})$ and $\mu_n^{qp}(e^{i\vartheta})$; and (b) calculating the Fourier integrals. The FFT technique (Cooley and Tukey 1965) is employed to accelerate the Fourier integrals.

One of the key steps that ensure the success of the above iterative solution algorithm is to represent with Fourier series the boundary forces/displacements on each crack surface. This technique is not new, and it is widely used to study the problem with periodic boundary values, e.g. the cylindrical shells with openings or nozzles (Xue et al. 2004, 2005) and composite materials with inclusions (Kushch et al. 2005).

3.5 The stress intensity factors (SIFs)

Andersson (1969) presented a formula to calculate the SIFs of a crack from its complex potentials. Specially, the SIFs at the tips of the p -th crack can be expressed as

$$k_I^p(\zeta_{tip}) - ik_{II}^p(\zeta_{tip}) = 2\sqrt{\pi} \frac{\varphi'_p(\omega_p(\zeta_{tip}))\omega'_p(\zeta_{tip})}{[e^{i\delta}\omega''_p(\zeta_{tip})]^{1/2}}, \tag{18}$$

where $\zeta_{tip} = \pm 1$ is the coordinates at the crack tips in ζ -plane, and $\delta = \theta_p$ is the angle between the x -axis and the tangent to the crack at its tips

After solving the unknowns A_n^p , the function $\varphi'_p(\omega_p(\zeta))$ can be obtained from Eq. 11a. Substituting $\varphi'_p(\omega_p(\zeta))$ into Eq. 18 yields

$$k_I^p(\pm 1) - ik_{II}^p(\pm 1) = 2\sqrt{\frac{\pi}{d_p}} \sum_{n=1}^{\infty} A_n^p(\pm 1)^{-n-1}, \tag{19}$$

which defines, in terms of the constants A_n^p , the SIFs of at the tips of the p -th crack.

3.6 The crack opening displacements (COD)

The COD, which plays an important role in predicting the effective moduli of cracked solids (see [Kachanov 1993](#)), denotes the displacement difference between the top and bottom surfaces of a crack. According to Eqs. 1a, 2 and 9, the displacement fields in a cracked solid are represented by functions $\varphi_q(z)$ and $\psi_q(z)$, where $1 \leq q \leq N$. However, the COD of the p -th crack is solely determined by functions $\varphi_p(z)$ and $\psi_p(z)$. This is because on the top and bottom surfaces of the p -th crack, the displacements induced by other functions $\varphi_q(z)$ and $\psi_q(z)$ where $q \neq p$ are continuous and hence the COD contributed by these functions is zero.

On the p -th crack, the displacement induced by $\varphi_p(z)$ and $\psi_p(z)$ is

$$2G(u_x^p + iu_y^p) = \kappa\varphi_p(z) - \overline{z\varphi'_p(z)} - \overline{\psi_p(z)}. \tag{20}$$

Substituting $\Omega(z; \theta_p, z_p^0, \varphi_p, \psi_p)$ (6) into the above expression to eliminate the function $\psi_p(z)$ yields

$$2G(u_x^p + iu_y^p) = \kappa\varphi_p(z) - e^{2i\theta_p} \overline{\Omega(z; \theta_p, z_p^0, \varphi_p, \psi_p)} + \left[z - z_p^0 - e^{2i\theta_p} \overline{(z - z_p^0)} \right] \overline{\varphi'_p(z)}. \tag{21}$$

Noting that $z - z_p^0 - e^{2i\theta_p} \overline{(z - z_p^0)} = 0$ for z lying on the p -th crack segment, the above displacement can be further simplified into

$$2G(u_x^p + iu_y^p) = \kappa\varphi_p(\omega_p(e^{i\vartheta})) - e^{2i\theta_p} \overline{\Omega(\omega_p(e^{i\vartheta}); \theta_p, z_p^0, \varphi_p, \psi_p)}, \tag{22}$$

which represents the displacement on the top surface when $0 \leq \vartheta \leq \pi$ and the displacement on the bottom surface when $\pi \leq \vartheta \leq 2\pi$, respectively.

Multiplying $\omega_p(\zeta)$ to both sides of Eq. (11) and integrating with respect to ζ yields

$$\varphi_p(\omega_p(\zeta)) = -e^{i\theta_p} \sum_{n=1}^{\infty} \frac{A_n^p}{n} \zeta^{-n} + C_0, \tag{23a}$$

$$\Omega(\omega_p(\zeta); \theta_p, z_p^0, \varphi_p, \psi_p) = -e^{i\theta_p} \sum_{n=1}^{\infty} \frac{B_n^p}{n} \zeta^{-n} + C_1, \tag{23b}$$

where C_0 and C_1 are complex constants. Therefore, after substituting $\zeta = e^{i\vartheta}$ and Eq. (23) into Eq. (22), the COD of the p -th crack is obtained as

$$\Delta u_x^p + i\Delta u_y^p = \frac{e^{i\theta_p}}{2G} \sum_{n=1}^{\infty} \left(\kappa \frac{A_n^p}{n} + \frac{\overline{B_n^p}}{n} \right) (e^{in\vartheta} - e^{-in\vartheta}), \quad 0 \leq \vartheta \leq \pi, \tag{24}$$

where ϑ denotes the position on the crack.

It is noticed that the COD varies along the crack, and its average value is

$$\langle \Delta u_x^p \rangle + i \langle \Delta u_y^p \rangle = \frac{1}{2d_p} \int_{L_p} (\Delta u_x^p + i \Delta u_y^p) |dz|. \tag{25}$$

According to Eq. (3), $dz = -e^{i\theta_p} d_p \sin \vartheta d\vartheta$ holds on the p -th crack. Then, substituting Eq. (24) into Eq. (25), the average COD can be expressed as

$$\langle \Delta u_x^p \rangle + i \langle \Delta u_y^p \rangle = i \frac{e^{i\theta_p}}{2G} \int_0^\pi \sum_{n=1}^\infty \left(\kappa \frac{A_n^p}{n} + \frac{\overline{B_n^p}}{n} \right) \sin(n\vartheta) \sin \vartheta d\vartheta. \tag{26}$$

Simplifying the integration in the right-side of the above equation yields

$$\langle \Delta u_x^p \rangle + i \langle \Delta u_y^p \rangle = i \frac{\pi e^{i\theta_p}}{4G} \left(\kappa A_1^p + \overline{B_1^p} \right). \tag{27}$$

This is the final expression of the average COD of the p -th crack.

4 Results and discussion

The algorithm described in Sect. 3.4 is implemented with FORTRAN on a PC system with an Intel Xeon 5130 dual-core CPU, and FFT is employed to accelerate the integration in Eq. (16).

4.1 Two collinear cracks under uniform normal stress at infinity

To demonstrate the efficiency of the proposed method, a simple example with two collinear cracks under uniform normal stress at infinity is considered. The geometric configuration is shown in Fig. 2, where a and h denote respectively the half-length of the crack and the half-distance between the two cracks.

In Table 1, the dimensionless SIFs of tip A and tip B are calculated and compared with the results obtained by other researchers including the exact solution (Sneddon 1969), the Kachanov solution (Kachanov 1987) and the modified Kachanov solution (Li et al. 2003). It is observed that in terms of computational accuracy, the new method provides a very accurate approximate solution virtually the same as the exact one after only ten iterations for which the CPU time is less than 0.03 seconds; also, it converges very fast such that the results obtained after only two iterations are already comparable with the well known Kachanov method. Moreover, unlike the other two methods whose accuracy decreases significantly as the cracks getting close to each other, the performance of the new method is insensitive to the distance between cracks and it can be used to effectively solve interactions between closely-spaced cracks.

The average COD of cracks plays an important role in predicting the effective moduli of cracked solids, see, for example, Kachanov (1993). In Table 2, the dimensionless average COD of the crack is calculated and compared with the exact solution (Sneddon 1969). Again, good agreement and fast convergence is observed. It is interesting to note that the accuracy of the average COD is better than the SIFs.

The CPU time of the proposed method depends on several internal parameters in the FORTRAN code: (a) the data length of FFT algorithm, which is 2^6 in this case; and (b) the

Fig. 2 Configuration of two collinear cracks

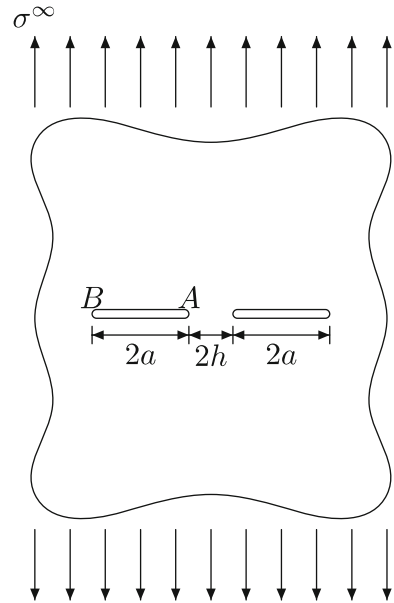


Table 1 The dimensionless SIFs K_I (normalized by $\sigma^\infty \sqrt{\pi a}$) of tip A and tip B

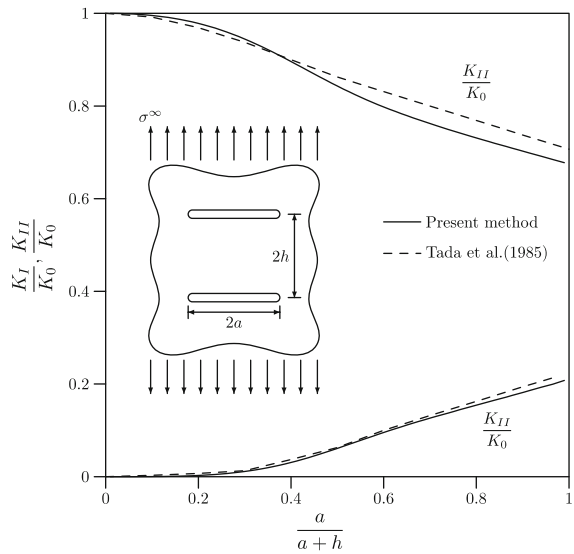
Iterative step	$h/a = 0.1$			$h/a = 0.01$		
	K_I^A	K_I^B	Err. (%)	K_I^A	K_I^B	Err. (%)
0	1.00000	1.00000	33	1.00000	1.00000	67
1	1.38066	1.09752	7.4	2.00977	1.12916	33
2	1.46768	1.11685	1.6	2.55581	1.17365	15
3	1.48637	1.12093	0.3	2.80618	1.19197	6.6
4	1.49035	1.12180		2.91641	1.19982	2.9
5	1.49120	1.12199		2.96448	1.20323	1.3
6	1.49138	1.12203		2.98538	1.20471	0.6
7	1.49142	1.12204		2.99447	1.20535	
8	1.49143	1.12204		2.99842	1.20564	
9	1.49143	1.12204		3.00014	1.20575	
10	1.49143	1.12204		3.00089	1.20581	
CPU-Time(S)	0.020			0.028		
Exact	1.49143	1.12204		3.00442	1.20581	
Kachanov	1.46891	1.12013	1.5	2.49600	1.19114	17
Modified Kachanov	1.49844	1.12493	0.5	2.89529	1.22225	3.6

effective length the output data after FFT, which is controlled by a tolerance (10^{-6} in this case) for the relative error defined between the normal of output data and the normal of the sequence $\{A_n^{p(m)}\}_{n \geq 1}$ and $\{B_n^{p(m)}\}_{n \geq 1}$.

Table 2 The dimensionless average COD (normalized by $\frac{(\kappa+1)\pi}{8G}\sigma^\infty a$)

Iterative step	$h/a = 0.1$		$h/a = 0.01$	
	Δu_y	Err. (%)	Δu_y	Err. (%)
0	1.00000	17	1.00000	29
1	1.16673	3.6	1.24949	12
2	1.20135	0.7	1.34507	5
3	1.20871		1.38538	2.2
4	1.21027		1.40277	0.9
5	1.21061		1.41032	
6	1.21068		1.41360	
7	1.21069		1.41502	
8	1.21070		1.41564	
9	1.21070		1.41591	
10	1.21070		1.41603	
Exact	1.21070		1.41612	

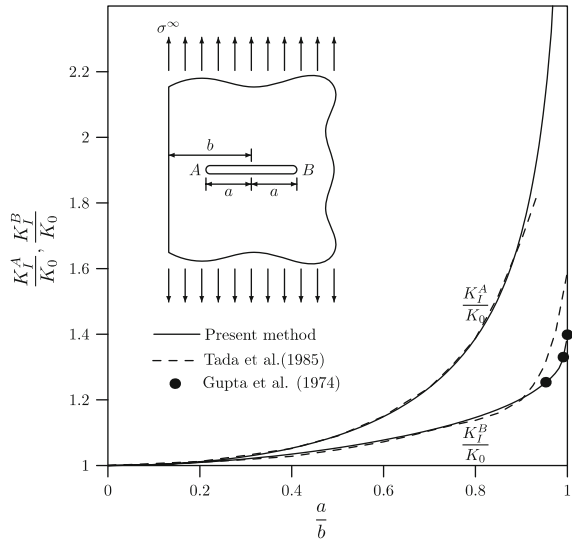
Fig. 3 Comparison of K_I and K_{II} normalized by K_0 ($K_0 = \sigma^\infty \sqrt{\pi a}$) for two parallel cracks under uniform normal stress at infinity



4.2 Two parallel cracks under uniform normal stress at infinity

As shown in Fig. 3, this example considers two parallel cracks under uniform normal stress at infinity. The lengths of the two cracks are both $2a$ and the distance between them is $2h$. The SIFs K_I and K_{II} are normalized by $K_0 = \sigma^\infty \sqrt{\pi a}$. Then, the dimensionless SIFs K_I/K_0 and K_{II}/K_0 obtained by the proposed method are compared with the results reported by Isida (1972) (see also Tada et al. 1985). The two curves plotted in Fig. 3 illustrate the relation between the geometric configuration of cracks, which is described by a scalar factor $a/(a + h)$, and the dimensionless SIFs. It is observed that the results obtained with the new method agree reasonably well with the verified existing results.

Fig. 4 Comparison of K_I normalized by K_0 ($K_0 = \sigma^\infty \sqrt{\pi a}$) for half-plane including internal crack under uniform tensile stress at infinity



4.3 Half-plane including cracks under tension

This example considers a crack in a half-plane under tensile stress at infinity. As shown in Fig. 4, the length of the crack is $2a$, and the distance between the crack center and the free surface is b . The half-plane problem can be easily solved with the proposed method and with minor modifications. Specifically, the conformal mapping in Eq. 3 is replaced by

$$\omega_0(\zeta) = -ie^{i\theta_0}d_0 \frac{\zeta + 1}{\zeta - 1} + z_0, \tag{28}$$

where θ_0 is the angle between the free surface of the half-plane and the x -axis, z_0 indicates a fixed point on the free surface, and d_0 is an arbitrary real constant. The conformal mapping Eq. 28 maps the half-plane in the z -plane to the exterior of the unit circle in the ζ -plane and induces formally the same boundary condition and formally the same expression of the complex potentials as Eqs. 5, 6, 7, 8 and the only difference is the replacement of θ_p and z_p^0 with θ_0 and z_0 .

The two curves plotted in Fig. 4 illustrate the relation between the geometric configuration described by a/b and the dimensionless SIFs K_I/K_0 and K_{II}/K_0 . The results obtained with the proposed method are compared with the results reported by Tada et al. (1985) and Gupta and Erdogan (1974). Although the three results agree well in most of the region, a visible difference between the new result and Tada’s result is observed when the internal crack is very close to the free surface. However, in this controversial area, the present result and Gupta’s result agree to each other perfectly.

4.4 Impact of the interaction of numerous cracks on effective moduli

The proposed method is able to efficiently and accurately solve interactions among a large number of cracks irregularly spaced in the whole/half plane. In this example, 2,500 cracks are randomly distributed on a 50×50 square lattice and are under tensile stresses at infinity. The effective Young’s modulus of the cracked solid is calculated and then compared with related results in the literatures.

When analysing the effective moduli of a cracked solid, the following formula is commonly used in the literature to compute the average strain, see e.g. [Kachanov \(1993\)](#),

$$\boldsymbol{\varepsilon} = \mathbf{M}_0 : \boldsymbol{\sigma}^\infty + \frac{1}{A} \sum_{p=1}^N d_p (\langle \mathbf{b} \rangle_p \mathbf{n}_p + \mathbf{n}_p \langle \mathbf{b} \rangle_p), \tag{29}$$

where \mathbf{M}_0 is the compliance tensor of the corresponding faultless material, $\boldsymbol{\sigma}^\infty$ the stress field at infinity, A the representative area, N the total number of cracks, d_p the half-length of the p -th crack, $\mathbf{n}_p = (-\sin \theta_p, \cos \theta_p)$ the unit normal vector of the p -th crack, $\langle \mathbf{b} \rangle_p = (\Delta u_x^p, \Delta u_y^p)$ the average COD vector of the p -th crack. After average COD $\langle \mathbf{b} \rangle_p$ on each crack surface is solved, the average strain can be readily computed according to Eq. (29), from which the effective elastic moduli of the cracked solid can be evaluated in connection with the stress field at infinity.

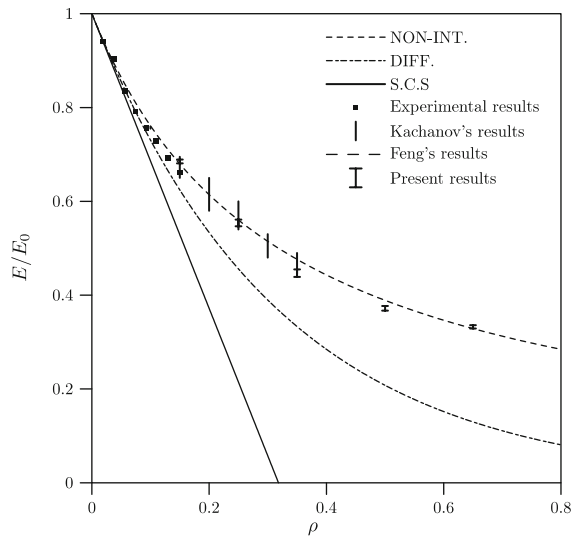
In this example, the cracked solid is treated as an isotropic solid, and the stresses at infinity satisfy conditions $\sigma_{yy}^\infty = 3\sigma_{xx}^\infty$ and $\sigma_{xy}^\infty = 0$. The effective Young’s modulus of the cracked solid is evaluated with the procedure described above, in which the average COD is obtained with the proposed method. Specially, five different densities $\rho \in \{0.15, 0.25, 0.35, 0.5, 0.65\}$ are investigated in this example, in which the crack density is defined as

$$\rho = \frac{1}{A} \sum_{p=1}^N d_p^2, \tag{30}$$

and for each specific density, ten sample crack arrays are randomly generated. In order to accurately capture the influence from crack interactions, the maximum iteration step for the calculation of average CODs is set as 10 in the computational experiments.

Figure 5 shows the relation between the crack density and the dimensionless Young’s modulus normalized by E_0 , the Young’s modulus of the corresponding faultless material. The results derived from different methods are compared in Fig. 5. As expected, the effective Young’s modulus in all the methods decreases as the crack density increases. It can be observed that the solutions from self-consistent scheme ([Budiansky and O’Connell 1976](#))

Fig. 5 Effective Young’s modulus of a cracked solid containing randomly spaced cracks. The result indicated by vertical bars, which represent the scatter of the results from all ten sample crack arrays, is from the proposed method; NON-INT. indicates the result from the approximate non-interacting scheme; DIFF indicates the result from the differential scheme; S.C.S indicates the result from the self-consistent scheme. For details, see, for example, [Kachanov \(1993\)](#). The experimental result ([Carvalho and Labuz 1996](#)), Kachanov’s results ([Kachanov 1993](#)) and Feng’s solution ([Feng et al. 2003](#)) are also replotted here



and the differential scheme (Hashin 1988) exhibit that the crack interaction is predicted to further reduce the stiffness of the cracked solids to yield a lower effective moduli than that without considering the crack interaction, however the prediction from the proposed method is very similar to that from the non-interacting model (Bristow 1960), even in the cases where the crack density is very high.

The underlying reasons for this are in two folds. Firstly, as addressed by Kachanov (1993), the interaction of randomly oriented cracks has two contrary effects on the cracked solid: (a) the crack shielding effect that strengthens the material, e.g. two parallel cracks shown in Sect. 4.1; and (b) the crack amplification effect that weakens the material, e.g. two collinear cracks shown in Sect. 4.2. In a solid containing a large number of randomly-distributed cracks, configurations resulting in crack shielding and crack amplification are both encountered, and as a result of the competition between the two opposite effects, the interaction among randomly-oriented cracks is not highlighted in affecting the effective moduli of the cracked solid. Secondly, the predictions of the self-consistent scheme and the differential scheme are insensitive to the mutual positions of cracks and the orientation of each individual crack that become increasingly more important as crack density grows. However, the proposed method accurately simulates the complicated and strong interaction among a large number of irregularly-distributed cracks, and consequently it is expected to give a more reliable prediction, especially for high crack densities.

The above analysis is partially supported by the result reported by Feng et al. (2003). Specifically, by combining the Kachanov's crack interaction method with the effective field method, Feng et al. (2003) proposed a simple method to analyze the strong interaction of a large number of randomly-distributed microcracks, in which the effect of the mutual position of cracks and the orientation of each individual crack are partly considered. As a result, the effective moduli from Feng's method are centered between the differential scheme and the non-interacting scheme in Fig. 5. Also, the experimental results (Carvalho and Labuz 1996) are in good agreement with the non-interacting theory, while the self-consistent scheme tends to overestimate the effective compliance. However, it should be mentioned that the cracked plate only contains 20 slots in the experimental study (Carvalho and Labuz 1996), and it may not be sufficient to represent a random distribution of cracks. Therefore, further experimental study for solids containing a larger number of cracks is of interest for assessing the accuracy of existing prediction schemes, in particular for high crack densities.

5 Conclusions

A fast and accurate method is presented in this paper to analyze interactions among cracks in linear elastic solids. The new method is developed for 2D problems, and its advantages over existing methods are in two folds: (a) the higher accuracy and efficiency in solving complicated crack interactions especially in problems where crack are closely spaced; (b) the capability to efficiently handle problems containing a large number of cracks. The performance of the proposed method is examined by a variety of benchmark results in the cracked solid. In many existing methods, the boundary conditions of cracks are equally transformed into a set of linear algebraic equations, and the accuracy and efficiency of these methods drop significantly as crack gets close. Until recently, few methods can be used to analyze a large number of cracks. However, in the proposed method, the unknowns are directly solved via their explicit expression of Fourier integrals, and by taking into account the mutual interaction between cracks through a perturbation approach, the accuracy of the solution is continuously improved with a fast iterative algorithm. Hence, the performance of the new method is

insensitive to the crack distribution and can effectively solve problems with a large number of cracks.

Acknowledgements This work is supported by the Research Grants Council of Hong Kong Special Administrative Region of China under the PolyU 5189/07E project and the research grant BB90 of the Hong Kong Polytechnic University.

Appendix: Interacting functions $\eta_n^{qp}(\zeta)$, $\mu_n^{qp}(\zeta)$, $\chi_n^{qp}(\zeta)$

The interactions between cracks are completely described by complex functions ϕ'_q and Ω' . In Eq. 11, functions ϕ'_q and Ω' are defined in ζ -plane corresponding to the q -th crack, and equivalently, they can be represented in the z -plane as

$$\phi'_q(z) = \frac{e^{i\theta_q}}{\omega'_q \circ \omega_q^{-1}(z)} \sum_{n=1}^{\infty} A_n^q [\omega_q^{-1}(z)]^{-n-1}, \quad 1 \leq q \leq N, \quad (\text{A-1a})$$

$$\Omega'(z; \theta_q, z_q^0, \varphi_q, \psi_q) = \frac{e^{i\theta_q}}{\omega'_q \circ \omega_q^{-1}(z)} \sum_{n=1}^{\infty} B_n^q [\omega_q^{-1}(z)]^{-n-1}, \quad 1 \leq q \leq N. \quad (\text{A-1b})$$

where the notation “ \circ ” in the chains denotes the composition of functions. Substituting the conformal mapping $z = \omega_p(\zeta)$ corresponding to the p -th crack into the above equations yields

$$\phi'_q(\omega_p(\zeta)) = \frac{e^{i\theta_q}}{\omega'_q \circ \omega_q^{-1} \circ \omega_p(\zeta)} \sum_{n=1}^{\infty} A_n^q [\omega_q^{-1} \circ \omega_p(\zeta)]^{-n-1}, \quad (\text{A-2a})$$

$$\Omega'(\omega_p(\zeta); \theta_q, z_q^0, \varphi_q, \psi_q) = \frac{e^{i\theta_q}}{\omega'_q \circ \omega_q^{-1} \circ \omega_p(\zeta)} \sum_{n=1}^{\infty} B_n^q [\omega_q^{-1} \circ \omega_p(\zeta)]^{-n-1}. \quad (\text{A-2b})$$

Equations A-2a describes the influence of ϕ' from the q -th crack to the p -th crack. Comparing Eqs. A-2a and 12a, the interaction function $\eta_n^{qp}(\zeta)$ can be determined as

$$\eta_n^{qp}(\zeta) = e^{i(\theta_q - \theta_p)} \zeta \omega'_p(\zeta) \frac{\tilde{\zeta}^{-n-1}}{\omega'_q(\tilde{\zeta})}, \quad (\text{A-3})$$

where

$$\tilde{\zeta} = \omega_q^{-1} \circ \omega_p(\zeta). \quad (\text{A-4})$$

Following the definition of complex potential Ω Eq. 6, $\Omega'(z; \theta_p, z_p^0, \varphi_q, \psi_q)$ is expressed as

$$\begin{aligned} \Omega'(z; \theta_p, z_p^0, \varphi_q, \psi_q) &= e^{2i(\theta_p - \theta_q)} \Omega'(z; \theta_q, z_q^0, \varphi_q, \psi_q) + (1 - e^{2i(\theta_p - \theta_q)}) \phi'_q(z) \\ &+ \left[\left(1 - e^{2i(\theta_p - \theta_q)}\right) z + \left(e^{2i(\theta_p - \theta_q)} z_q^0 - z_p^0\right) + e^{2i\theta_p} \right. \\ &\times \left. \left(\bar{z}_p^0 - \bar{z}_q^0\right) \right] \phi''_q(z), \end{aligned} \quad (\text{A-5})$$

where due to Eq. A-1a,

$$\phi''_q(z) = e^{i\theta_q} \sum_{n=1}^{\infty} A_n^q \frac{[\omega_q^{-1}(z)]^{-n-2}}{[\omega'_q \circ \omega_q^{-1}(z)]^2} \left[-n - 1 - \omega_q^{-1}(z) \frac{\omega''_q \circ \omega_q^{-1}(z)}{\omega'_q \circ \omega_q^{-1}(z)} \right]. \quad (\text{A-6})$$

Substituting Eqs. A-2b and A-6 into Eq. A-5 yields the influence of Ω' from the q -th crack to the p -th crack. Then, comparing with Eq. 12b, the interacting functions $\mu_n^{qp}(\zeta)$ and $\chi_n^{qp}(\zeta)$ can be determined as

$$\mu_n^{qp}(\zeta) = e^{2i(\theta_p - \theta_q)} \eta_n^{qp}(\zeta). \quad (\text{A-7})$$

$$\begin{aligned} \chi_n^{qp}(\zeta) = & \left(1 - e^{2i(\theta_p - \theta_q)}\right) \eta_n^{qp}(\zeta) + e^{i(\theta_q - \theta_p)} \zeta \omega_p'(\zeta) \frac{\tilde{\zeta}^{-n-2}}{[\omega_q'(\tilde{\zeta})]^2} \left[-n - 1 - \tilde{\zeta} \frac{\omega_q''(\tilde{\zeta})}{\omega_q'(\tilde{\zeta})} \right] \\ & \cdot \left[\left(1 - e^{2i(\theta_p - \theta_q)}\right) \omega_p(\zeta) + \left(e^{2i(\theta_p - \theta_q)} z_q^0 - z_p^0\right) + e^{2i\theta_p} \left(\bar{z}_p^0 - \bar{z}_q^0\right) \right]. \quad (\text{A-8}) \end{aligned}$$

References

- Andersson H (1969) Stress intensity factors at the tips of a star-shaped contour in an infinite tensile sheet. *J Mech Phys Solids* 17:405–414
- Benveniste V, Dvorak GJ, Zazour J et al (1989) On interacting cracks and complex crack configurations in linear elastic media. *Int J Solids Struct* 25:1279–1293
- Bristow JR (1960) Microcracks and the static and dynamic elastic constants of annealed and heavily cold-worked metals. *British J Appl Phys* 11:81–85
- Budiansky B, O'Connell RJ (1976) Elastic moduli of a cracked solid. *Int J Solids Struct* 12:81–97
- Carvalho FCS, Labuz JF (1996) Experiments on effective elastic modulus of two-dimensional solids with cracks and holes. *Int J Solids Struct* 33(28):4119–4130
- Chen WH, Chen TC (1995) An efficient dual boundary-element technique for a 2-dimensional fracture problem with multiple cracks. *Int J Numer Methods Eng* 38(10):1739–1756
- Cooley JW, Tukey JW (1965) An algorithm for the machine calculation of complex Fourier series. *Math Comput* 19:297–301
- Denda M, Dong YF (1997) Complex variable approach to the BEM for multiple crack problems. *Comput Meth Appl Mech Eng* 141:247–264
- Erdogan F (1962) On the stress distribution in plates with collinear cuts under arbitrary loads. In: proceedings of 4th U.S. national congress of applied mechanics, vol 1, ASME, pp 547–553
- Erdogan F (1969) Approximate solutions of systems of singular integral equations. *SIAM J Appl Math* 17(6):1041–1059
- Erdogan F, Gupta GD (1972) On the numerical solution of singular integral equations. *Q Appl Math* 29:525–534
- Feng XQ, Li JY, Yu SW (2003) A simple method for calculating interaction of numerous microcracks and applications. *Int J Solids Struct* 40:447–464
- Gupta GD, Erdogan F (1974) The problem of edge cracks in an infinite strip. *J Appl Mech Trans ASME* 41(4):1001–1006
- Hashin Z (1988) The differential scheme and its application to cracked materials. *J Mech Phys Solids* 36:719–734
- Isida M (1972) Method of Laurent expansion for internal crack problems. In: Sih GC (ed) *Methods of analysis and solutions of crack problems*. Martinus-Nijhoff, The Hague
- Kachanov M (1987) Elastic solids with many cracks: a simple method of analysis. *Int J Solids Struct* 23:23–45
- Kachanov M (1993) Elastic solids with many cracks and related problems. *Adv Appl Mech* 30:259–445
- Kachanov M (2003) On the problems of crack interactions and crack coalescence. *Int J Fract* 120:537–543
- Koiter WT (1959) An infinite row of collinear cracks in an infinite elastic sheet. *Ingenieur Archiv* 28:168–173
- Kushch VI, Shmegeva SV, Buryachenko VA (2005) Interacting elliptic inclusions by the method of complex potentials. *Int J Solids Struct* 42(20):5491–5512
- Li YP, Tham LG, Wang YH et al (2003) A modified Kachanov method for analysis of solids with multiple cracks. *Eng Fract Mech* 70:1115–1129
- Ma L, Wang XY, Feng XQ, Yu SW (2004) Numerical analysis of interaction and coalescence of numerous microcracks. *Eng Fract Mech* 72:1841–1865
- Muskhelishvili NI (1953a) Some basic problems of the mathematical theory of elasticity. P. Noordhof, Groningen
- Muskhelishvili NI (1953b) Singular integral equations. Noordhof, Groningen, The Netherlands

- Pan E (1997) A general boundary element analysis of 2-D linear elastic fracture mechanics. *Int J Fract* 88: 41–59
- Sih GC (1964) Boundary problems for longitudinal shear cracks. In: proceedings of 2nd conference on theoretical and applied mechanics. Pergamon, New York
- Sneddon IN, Lowengrub M (1969) Crack problems in the classical theory of elasticity. Wiley, New York
- Tada H, Paris PC, Irwin GR (1985) The stress analysis of cracks handbook. Paris Production and Del Reasearch Corporation, St. Louis
- Westergaard HM (1939) Bearing pressures and cracks. *J Appl Mech* 6:A49–A53
- Willmore TJ (1949) The distribution of stress in the neighborhood of a crack. *Q J Mech Appl Math* 2(1):53–64
- Xue MD, Li DF, Hwang KC (2004) Analytical solution of two intersecting cylindrical shells subjected to transverse moment on nozzle. *Int J Solids Struct* 41(24–25):6949–6962
- Xue MD, Li DF, Hwang KC (2005) Theoretical stress analysis of intersecting cylindrical shells subjected to external loads transmitted through branch pipes. *Int J Solids Struct* 42(11–12):3299–3319